Materials Research. 2011; 14(1): 124-133
DOI: 10.1590/S1516-14392011005000017

Grain Refinement of AZ91D Magnesium Alloy by $MgCO_3$

Ti Jun Chen*, Xiang Dong Jiang, Ying Ma, Rui Quan Wang, Yuan Hao

Key Laboratory of Gansu Advanced Nonferrous Metal Materials,
Lanzhou University of Technology, Lanzhou 730050, China

Received: January 1, 2011; Revised: February 22, 2011

The grain refining technique of AZ91D magnesium alloy by $MgCO_3$ has been investigated. The refining mechanism and tensile properties of the resulting alloy have also been discussed. The results indicate that $MgCO_3$ can decrease its grain size from 311 to 53μm. Correspondingly, the tensile properties are obviously improved. The higher the cooling rate from addition temperature to pouring temperature or the higher the addition temperature, the finer the grains. The melt treated by $MgCO_3$ should be poured as soon as possible because the inoculation fading is quite quick. The microstructure sensitivity to the diameter of a cast rod is relatively high and the microstructures of the rods with large diameters are quite inhomogeneous. The refining mechanism of $MgCO_3$ belongs to heterogeneous nucleation and the nucleant substrates are believed to be the Al_4C_3 particles formed from the reactions between the $MgCO_3$ and the molten alloy.

Keywords: *AZ91D magnesium alloy, grain refinement, $MgCO_3$, microstructure*

1. Introduction

Magnesium alloys have large potential in fabrication of structural components of automobiles due to their high specific strength[1]. In addition, they also have wide applications in the fields of electronic products, portable tools, sporting goods and aerospacevehicles[2]. However, the mechanical properties of most of them are relatively low compared with those of another category of light alloys, aluminium alloys, and can not match the requirements in many applications. It is well known that grain refinement is very effective for improving mechanical properties of most of alloys. Furthermore, a fine microstructure is also very important for the properties of semi-fabricated products, e.g., starting ingots for rolling and thixoforming[3].

Depending upon whether they are alloyed with Al, magnesium alloys can be classified into two groups: aluminium free and aluminium bearing[4]. The aluminium free alloys can be well refined by Zr containing refiners and the corresponding technique has been widely used in practice. But for the aluminium bearing alloys, there is no a reliable technique to be commercially used so far although several approaches have been developed[3]. These approaches mainly include five kinds, superheating[4-8], the Elfinal process[4-6,8], grain refinement by other additives[4,5,8-15], native refinement[4,16] and carbon inoculation[4,5,17-20]. By contrast, the carbon inoculation not only has good refining effect, but also has good adaptability to alloys' compositions or impurities' contents[4,5]. So it has large application potential and should be paid more attention. The critical step of this method is the introduction of carbon into magnesium alloy melts. Reported methods include, but are not limited to, graphite, paraffin wax, lampblack, organic compounds (C_2Cl_6 and C_6Cl_6), carbonates ($CaCO_3$ and $MgCO_3$), carbides (Al_4C_3, SiC, CaC_2), and bubbling the melts with CO, CO_2 and CH_4 gasses[4,5,17-20]. Among the lots of additives, $MgCO_3$ has some special advantages compared with the others, such as relatively low cost due to its abundant resources, low decomposition temperature and high carbon absorptivity due to its slow release speed of CO_2 gas (compared with the organic compounds and bubbling method). So $MgCO_3$ may be a suitable refiner in commercial use.

However, there is no reference to detailedly report how the refining parameters, such as addition amount, addition temperature, holding time at pouring temperature and cooling rate from addition temperature to pouring temperature, affect the grain sizes of magnesium alloys using $MgCO_3$ as refiner and what are the optimal parameters. In addition, the dimensions of cast ingots can affect the cooling rate during solidification, and thus the microstructure. But there is no reference to involve this. Furthermore, most of the existing references about carbon inoculation have focused on the refining mechanism and suggest that Al_4C_3 or Al_2CO particles formed from the reactions between the introduced C element and the molten alloys are the nucleant substrates of α-Mg crystals[4,5,17-20]. But there is no direct evidence to demonstrate it.

Therefore, in this paper, the effects of the refining parameters mentioned above on the grain size or microstructure of AZ91D alloy and the corresponding refining mechanism have been investigated using $MgCO_3$ as refiner. In addition, the microstructure uniformity of cast rods with different diameters and the tensile properties have been examined.

2. Experimental Procedure

The material used in this work is commercial AZ91D alloy and its composition is Mg-9.04Al-0.6Zn-0.31Mn (the percentages all refer to weight percentage). As mentioned above, five parameters, such as the addition amount of $MgCO_3$, addition temperature, cooling rate of the melt from addition temperature to pouring temperature, holding time at pouring temperature and rod diameter, were considered. The detailed parameters used in this work are shown in Table 1. The pouring temperature of 705 °C was employed. A quantity of AZ91D alloy was processed according to the sequence of remelting, adding $MgCO_3$, cooling to pouring temperature, holding and pouring, some cast rods were prepared. It should be noted that the molten alloy was protected by RJ-2 covering agent designed for magnesium alloys during experiments. The desired cooling rates were obtained in the light of the number and duration of opening furnace lid during cooling: the more the number and the longer the duration, the higher the cooling rate.

*e-mail: chentj1971@126.com

Some small specimens were cut from the above cast rods. They were finished and polished by standard metallographic technique and etched by aqueous solution containing glycerol, nitric acid, hydrochloric acid and acetic acid. Then they were observed on a Mef-3 optical microscope (OM). To delineate grain boundaries and quantitatively examine grain size, some small specimens with dimensions of Φ16 × 10 mm were solutionized at 420 °C for 8 hours, and then water quenched, also processed according to the above procedures for preparing metallographic specimen and observed on the OM again. The resulting images were analyzed by Image-Plus 5.0

Table 1. Grain refining parameters of AZ91D alloy by $MgCO_3$ used in this work.

Treatment parameters	Addition amount (wt. (%))	Addition temperature (°C)	Cooling rate ($°C \cdot s^{-1}$)	Holding time (minutes)	Rod diameter (mm)
Addition amount	0, 0.2, 0.4, 0.6, 0.8, 1.0, 1.2, 1.4	790	4.25	0	16
Addition temperature	1.0	650, 670, 690, 710, 730, 750, 770, 790	4.25	0	16
Cooling rate	1.0	790	4.25, 1.4, 0.45, 0.14	0	16
Holding time	1.0	790	0.14	0, 10, 20, 30	16
Rod diameter	1.0	790	4.25	0	16, 45, 70

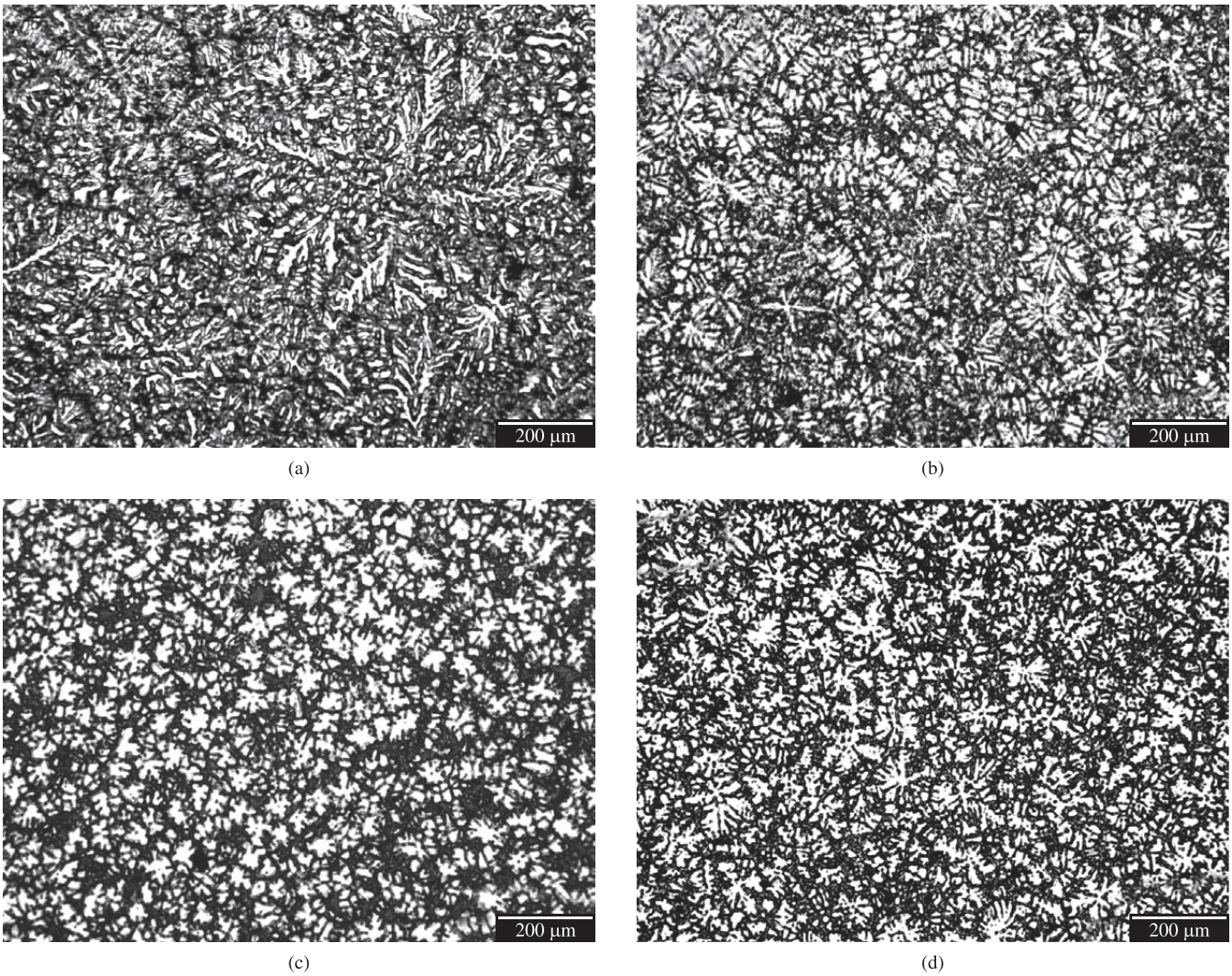

Figure 1. Microstructures of the AZ91D alloys refined by different amounts of $MgCO_3$. a) 0%; b) 0.6%; c) 1.0%; and d) 1.4%.

software. The diameter of a round having equivalent area to a grain is taken as the size of this grain. On each specimen, three typical images with magnification of 100 times were examined. The average value is taken as the grain size of this specimen. To verify the grain refining mechanism, the specimen refined by 1 % $MgCO_3$ were analyzed by electron microprobe analyzer (EPMA).

Based on the above experiments, a grain refining technique can be developed. To examine the tensile properties of the refined alloy, some ingots with 16 mm diameter were prepared according to this technique and machined into tensile testing bars with a gauge of 40 mm and a diameter of 8 mm. The tensile testing was carried out on a universal material testing machine at a nominal strain rate of $3.32 \times 10^{-3}s^{-1}$. The average of five tests was taken as the final properties (ultimate tensile strength (UTS) and elongation). Fracture surface morphologies and microstructures taken near the fracture surface along the tensile loading direction were observed on a scanning electron microscope (SEM) and the OM respectively. To verify the effect of refinement on the size of β phase, both the refined and un-refined alloys were also observed on the SEM.

3. Results and Discussion

3.1. Effects of grain refining parameters on microstructure

3.1.1. Effect of addition amount of $MgCO_3$

Figure 1 presents the typical microstructures of the AZ91D alloys refined by different amounts of $MgCO_3$. It indicates that the primary dendrites of the un-refined alloy are very developed (Figure 1a). After being treated by a little amount of $MgCO_3$, the dendrites are significantly refined and the refining effect is enhanced as the addition amount increases (comparing Figure 1b and c). Figure 1c shows that a microstructure with very fine and uniform equiaxed dendrites is obtained when the amount increases to 1%. But when the amount exceeds 1%, the dendrites slowly become developed again (comparing Figure 1c and d). This variation of grain size with addition amount can be more clearly seen from the microstructures of the solutionized alloys shown by Figure 2. It is worth noting that the microstructure is really fine and uniform after being treated by

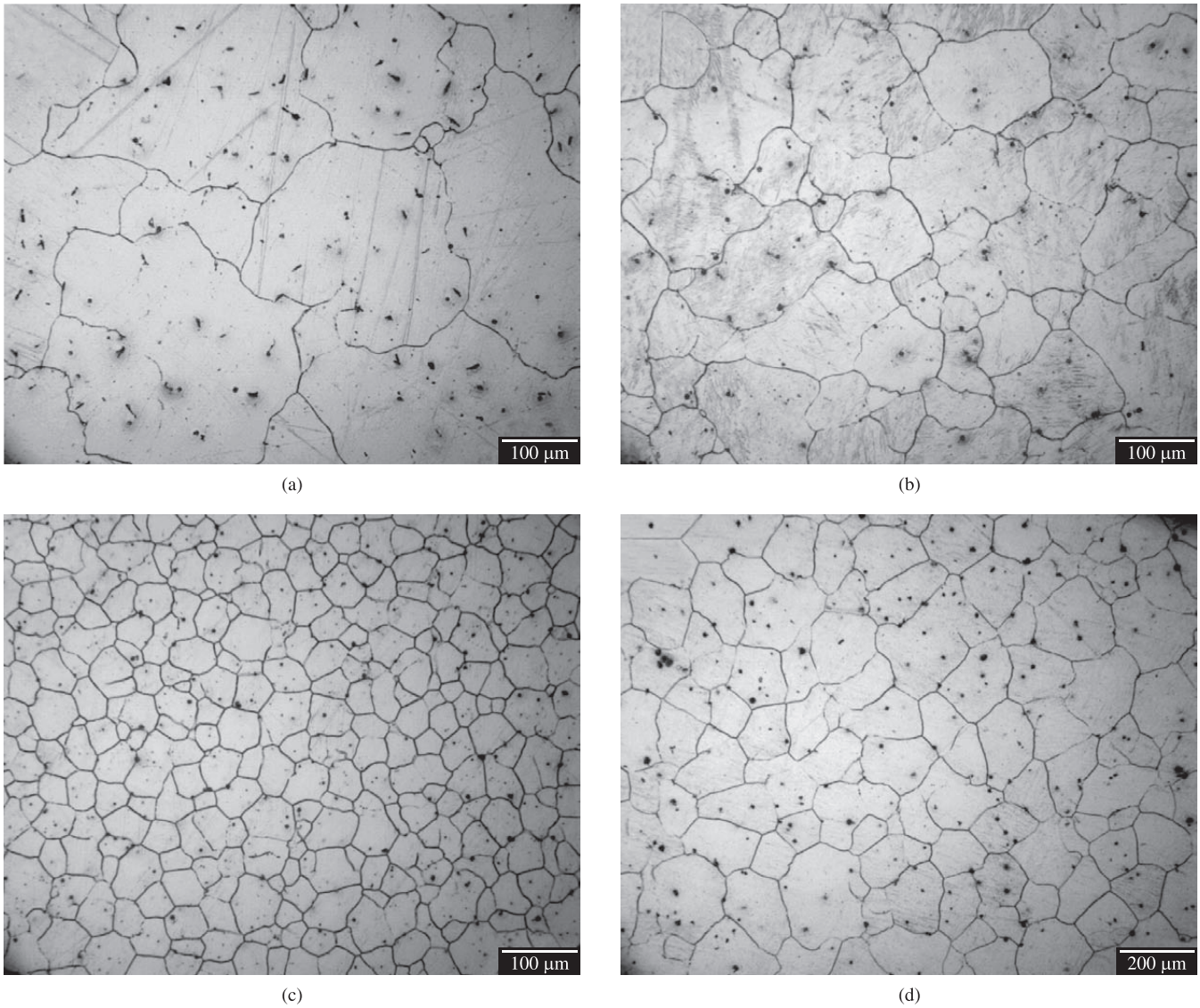

Figure 2. Microstructures of the AZ91D alloys shown in Figure 1 after being solution-treated at 420 °C for 8 hours.

1% $MgCO_3$ (Figure 2c). The quantitative examination result indicates that its grain size is only 53 μm, but that of the un-refined alloy is up to 311 μm (Figure 3), which means that $MgCO_3$ is an effective grain refiner for AZ91D alloy.

The popularly accepted mechanism of carbon inoculation is the heterogeneous nucleation taking Al_4C_3 particles as nucleant substrates[4,5,17-20]. The Al_4C_3 particles form from the reaction between the introduced C and the Al in the molten alloy. It can be expected that the number of nucleant substrates should increase as the $MgCO_3$ amount increases. But when the number exceeds a given limiting value, the frequency of mutual collision and coalescence of the Al_4C_3 particles may sharply increase. Moreover, the density of Al_4C_3 is higher than that of the molten alloy[21] and the coalescence may accelerate their settlement. Both the coalescence and settlement decrease the number of effective nucleant substrates. Therefore, the grain size first decreases as the addition amount of $MgCO_3$ increases and then instead becomes large when the amount exceeds a given value. The present results indicate that 1% is the appropriate addition amount. Figure 3 also shows that the change trend of grain size is not uniform with the addition amount. The decrease magnitude is relatively small between 0.2~0.6% additions. This should be attributed to the difference in carbon absorptivity or carbon loss resulted from some operating errors during experiment.

3.1.2. Effect of addition temperature

Figure 4 presents the variation of grain size with addition temperature of $MgCO_3$. It shows that the grain size continuously decreases as the temperature rises. As discussed in the above section, the nucleant substrates may be the Al_4C_3 particles formed from the reaction between the introduced C and the Al in the melt. It is well known that $MgCO_3$ will decompose into CO_2 and MgO at elevated temperature and rising the temperature can accelerate its decomposition. The C element that is needed by forming Al_4C_3 should result from the released CO_2 gas. So it can be expected that the temperature rise can enhance the formation of Al_4C_3 particles and increase their number to some extent, and thus leads the grain size to decrease.

In addition, when the melt temperature is properly elevated, some of the existing large-sized nucleant substrates may partially melt and one substrate possibly separate into two or more small-sized substrates[22], i.e., proper rising the melt superheating can increase the number of nucleant substrates. Furthermore, the superheating mechanism will play more and more obvious role as the temperature rises within a proper range[6]. Both these two regimes thereby can also decrease the grain size. But to reduce oxidation during melting, the addition temperature should be as low as possible according to the requirement for grain size.

3.1.3. Effect of holding time

Figure 5 gives the variation of grain size with holding time at the pouring temperature of 705 °C. It shows that the grain size continuously increases as the holding time is prolonged. As discussed above, the nucleant substrates may coarsen and settle. So it can be expected that the longer the holding time, the less the number of effective nucleant substrates, and thus the larger the resulting grains. It is known that the inoculation fading is a common phenomenon during grain refinement. Figure 5 indicates that the grain size increases from 124 to 226 μm after the treated melt is held for 30 minutes and the increase rate is quite high all along during the whole holding period. So the inoculation fading of the used $MgCO_3$ refiner is obvious and the melt should be poured as soon as possible after the melt is treated.

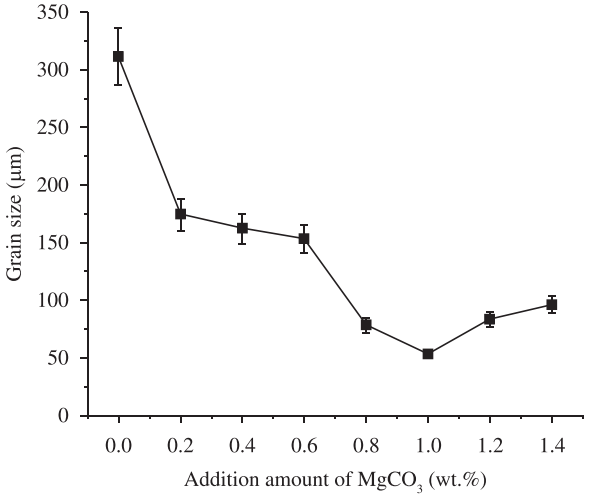

Figure 3. Variation of grain size with addition amount of $MgCO_3$.

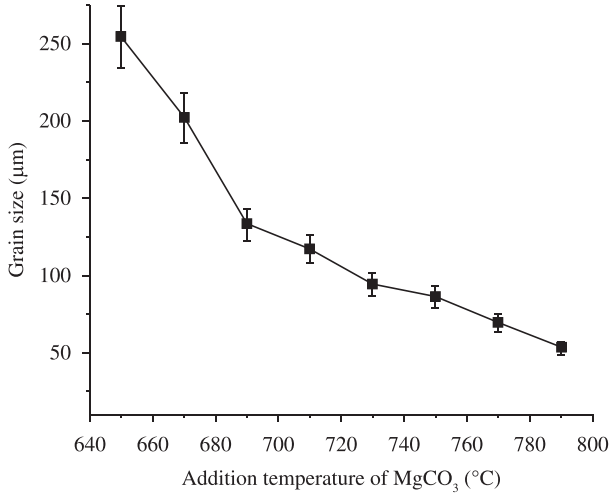

Figure 4. Variation of grain size with addition temperature of $MgCO_3$.

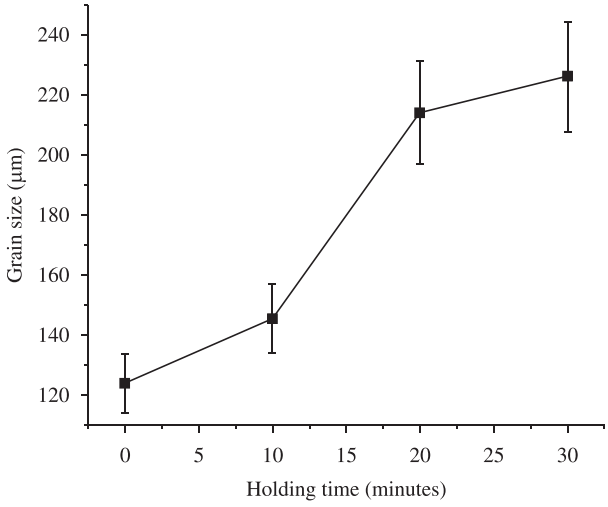

Figure 5. Variation of grain size with holding time.

3.1.4. Effect of cooling rate

Figure 6 shows the variation of grain size with cooling rate from the addition temperature of 790 °C to the pouring temperature of 705 °C. It indicates that the grain size decreases as the cooling rate increases. It can be suggested that the high cooling rate shortens the time for the coalescence and settlement of nucleant substrates, and thus increases the number of effective substrates and decreases the grain size. Furthermore, the melt is poured into steel mould with ambient temperature when it is cooled to 705 °C during experiment. The cooling rate after pouring should be relatively high and this high cooling rate can be further enhanced by the high cooling rate from addition temperature to pouring temperature. The high cooling rate after pouring must result in high supercooling degree of the melt, and thus refines the microstructure[23]. In other words, the effect of the cooling rate on supercooling degree is another reason why the grain size decreases as the cooling rate increases. Therefore, it can be suggested that the cooling rate should be improved as possible as one can.

3.1.5. Effect of cast rod diameter

Figure 7 presents the variation of grain size with cast rod diameter. It shows that the grain size increases with increasing the diameter. It should be noted that the grain size of each rod is the average of grain sizes in the center and edge zones of the rod. In fact, the rod diameter mainly affects the melt cooling rate during solidification: the larger the diameter, the lower the cooling rate and thus the larger the grains. Figure 7 indicates that the grain size increases from 53 μm to 140 μm when the rod diameter increases from 16 to 70 mm, i.e., the grain size increases about 2 times as the diameter increases 3 times, which implies that the microstructure sensitivity to casting thickness is relatively high for the AZ91D alloy treated by $MgCO_3$.

To examine the microstructure uniformity of the cast rods, the microstructures of two regions, the center and edge regions of each rod, are observed. Figure 8 gives the microstructures of the rods with different diameters. It shows that for the rod with 16 mm diameter, the microstructure is quite uniform and the difference between these two regions is very little (comparing Figure 8a and b). As the diameter enlarges, the grain sizes of these two regions all increase. But the increase extent in the edge region is smaller than that in the center region, i.e., the difference between these two regions becomes larger and larger as the diameter increases (Figure 8a-f). These changes can be more clearly seen from the quantitative examination result shown by Figure 9, which should be attributed to the difference in cooling rate between these two regions: the cooling rate of the edge region is higher than that of the center region and the difference between these two regions becomes large as the diameter increases. But it can be expected that as the diameter increases to a given degree, the temperature that the mould can be heated to during solidification will reach a limiting value and no more rises as the diameter further increases. Namely, the cooling rate in the melt close to mould wall (the edge regions of the cast rods) will not obviously change with the diameter. Thus, there has no large difference between the resulting microstructures. As shown by Figure 8d, 8f and Figure 9, the grain sizes in the edges are nearly same for the rods with diameters of 45 and 70 mm. But in the center regions, the cooling rate closely depends on the whole heater released after pouring and during solidification, and the heater increases as the liquid amount increases, i.e., as the diameter enlarges. So it is found that the grain size of the rod with 70 mm diameter is obviously larger than that of the rod with 45 mm diameter (comparing Figure 8c and e or the corresponding values in Figure 9).

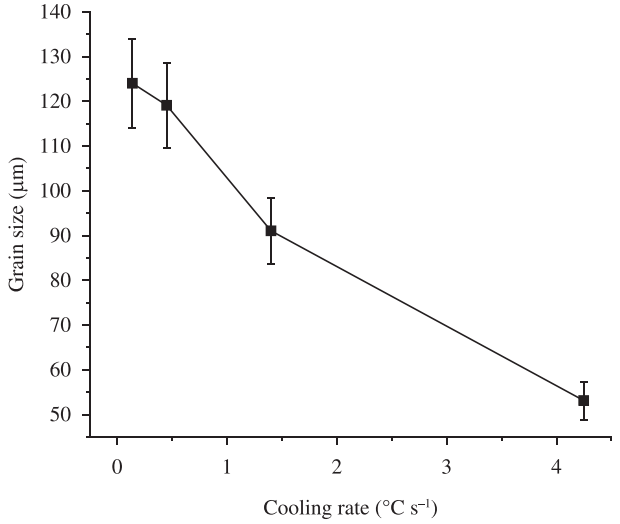

Figure 6. Variation of grain size with cooling rate from the addition temperature of 790 °C to pouring temperature of 705 °C.

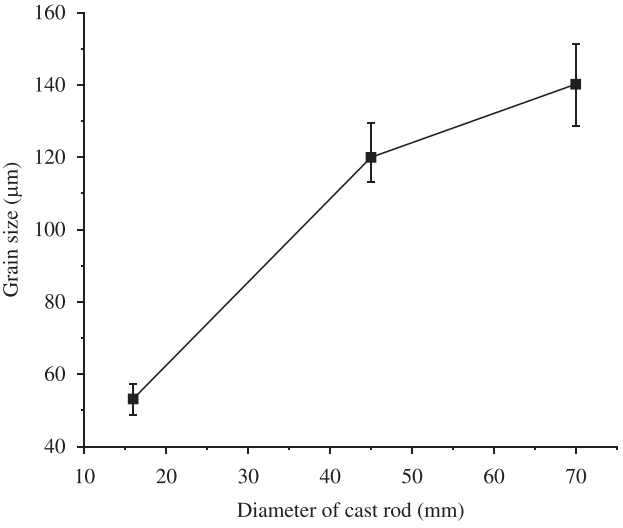

Figure 7. Variation of grain size with diameter of cast rod.

3.2. Grain refining mechanism of $MgCO_3$

For carbon inoculation of aluminium bearing magnesium alloys, the most commonly accepted mechanism is heterogeneous nucleation and the possible nucleant substrates include Al_4C_3 and Al_2CO particles[4,5,17-20,24,25]. When SiC particles are taken as refiner, it is suggested that the SiC particles themselves can also act as the substrates besides these two kinds of particles[17,18]. In addition, an investigation has proposed that C diffuses out from the α-Mg during solidification and then generates a constitutional undercooling region, which not only prevents the α-Mg grains from growth, but also can cause the formation of new nuclei[26]. However, the investigation from Qian et al. shows that only Mg-Al alloy can be refined when pure Mg, Mg-Zn and Mg-Al contain same amount of C (20 ppm) and thus disproves this standpoint[20]. From most of the recent investigations, it can be found that the actual nucleant substrates are Al_4C_3 particles, but not Al_2CO particles[16,24,25]. Unfortunately, there is no direct evidence to support this mechanism so far. So in the present work, EPMA analysis has been carried out to provide some evidences support this mechanism.

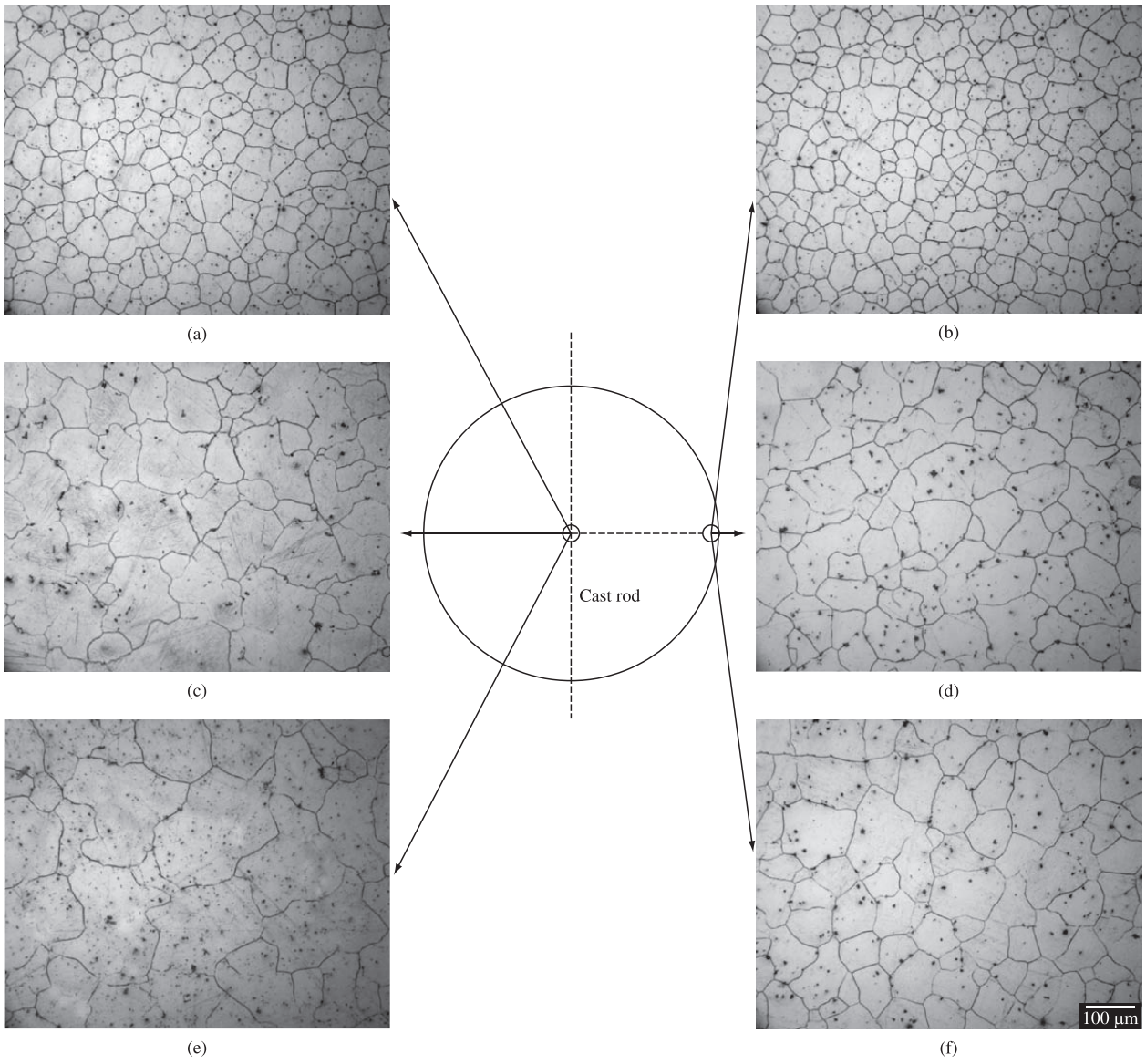

Figure 8. Microstructures of different regions of the refined AZ91D rods with different diameters solution treated at 420 °C for 8 hours. a-b) 16 mm; c-d) 45 mm; and e-f) 70 mm.

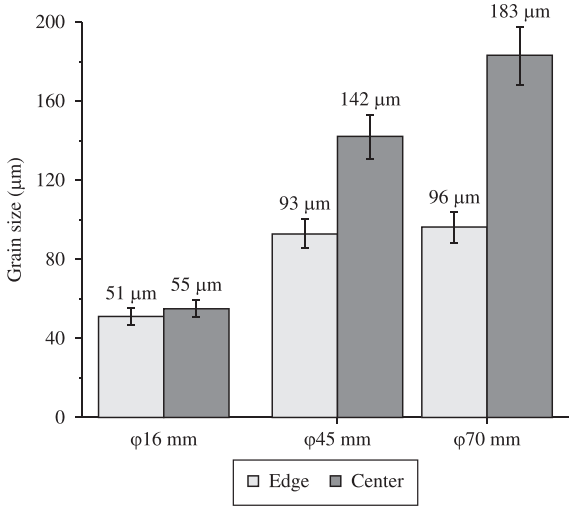

Figure 9. Grain sizes of different regions of the refined AZ91D rods with different diameters.

The present result shows that a small particle always exists in the center of each equiaxed dendrite (marked by arrow in Figure 10a) and it may be the nucleus of this dendrite. The EPMA results indicate that this particle is rich in Al and C (Figure 10b and c) and is composed of Mg, Al and C (Figure 11). It is believed that the Mg element should be resulted from the magnesium matrix[27] and the actual constituents only include the two elements of Al and C.

It is known that $MgCO_3$ will decompose into CO_2 and MgO when the temperature is higher than 420 °C through the reaction[28]:

$$MgCO_3 = CO_2 + MgO$$
$$(\Delta G = 117458 - 169.708\ T\ (298\sim1000K)) \quad (1)$$

The released CO_2 gas then reacts with Mg in the melt and C is reduced according to the reaction:

$$CO_2 + 2Mg = C + 2MgO \quad (2)$$

The existing investigation indicates that Mg can react with CO_2 to form C at above 400 °C[29]. Finally, the reduced C reacts with Al in the melt to form the Al_4C_3 particles through the reaction[30]:

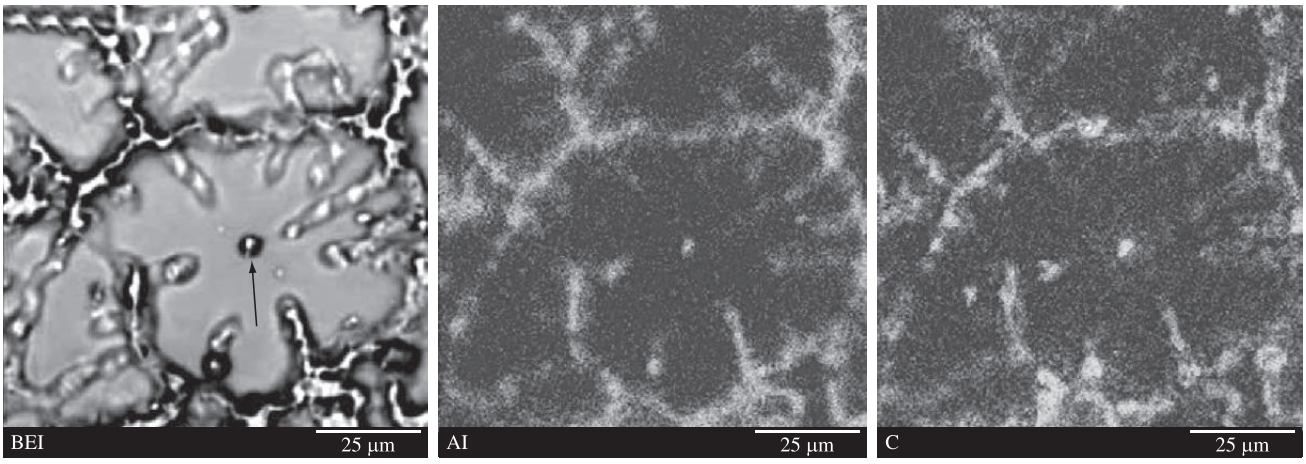

Figure 10. a) Back scattered electron imaging micrograph; b) Al and; c) C maps of the alloy refined by 1% $MgCO_3$.

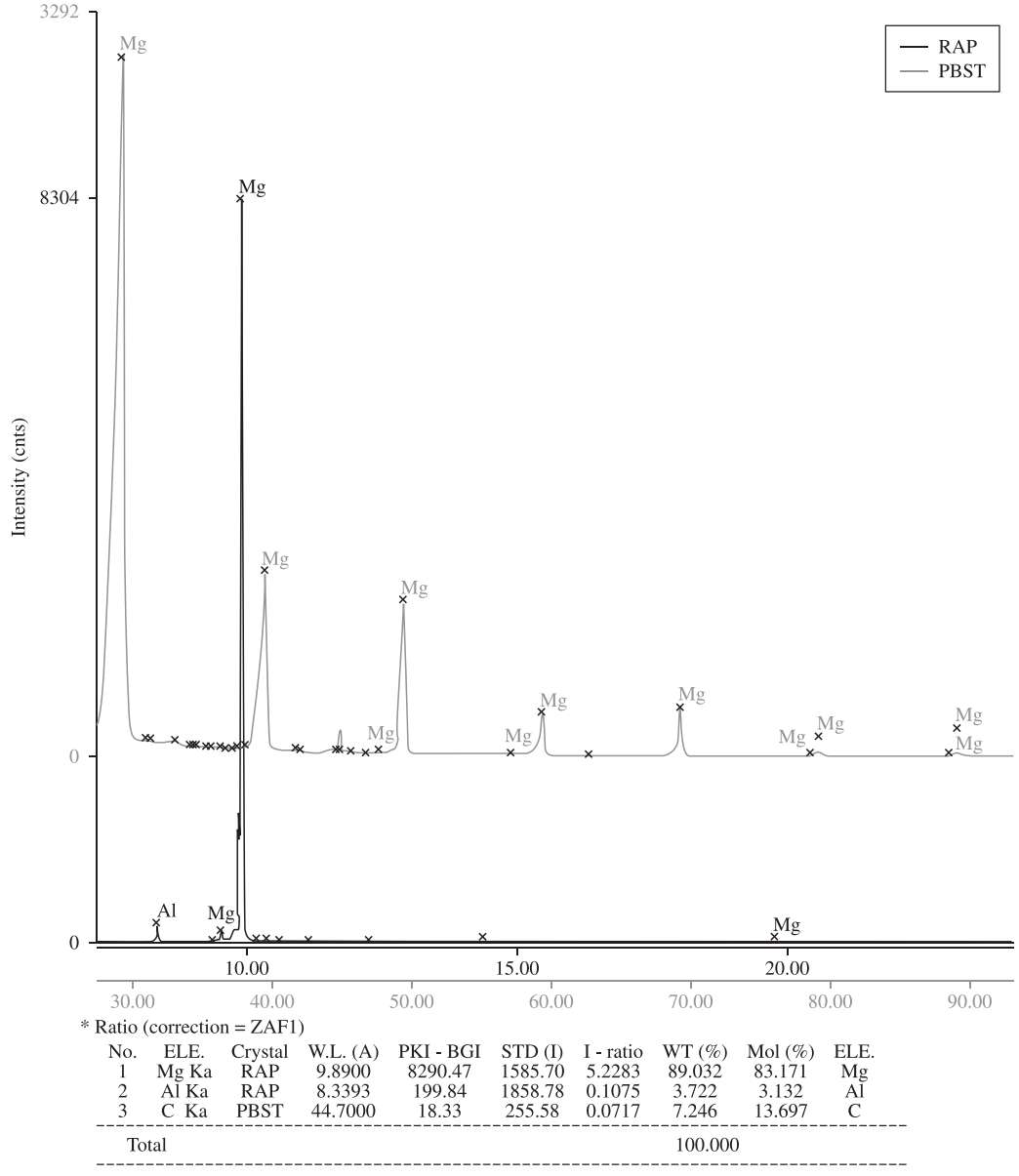

* Ratio (correction = ZAF1)

No.	ELE.	Crystal	W.L. (A)	PKI - BGI	STD (I)	I - ratio	WT (%)	Mol (%)	ELE.
1	Mg Ka	RAP	9.8900	8290.47	1585.70	5.2283	89.032	83.171	Mg
2	Al Ka	RAP	8.3393	199.84	1858.78	0.1075	3.722	3.132	Al
3	C Ka	PBST	44.7000	18.33	255.58	0.0717	7.246	13.697	C
Total							100.000		

Figure 11. EPMA result of the point shown by arrow in Figure 10.

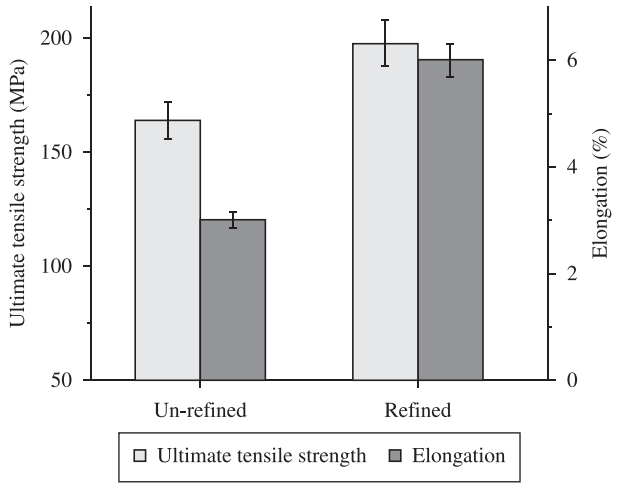

Figure 12. Ultimate tensile strength and elongation of the AZ91D alloys with and without refinement.

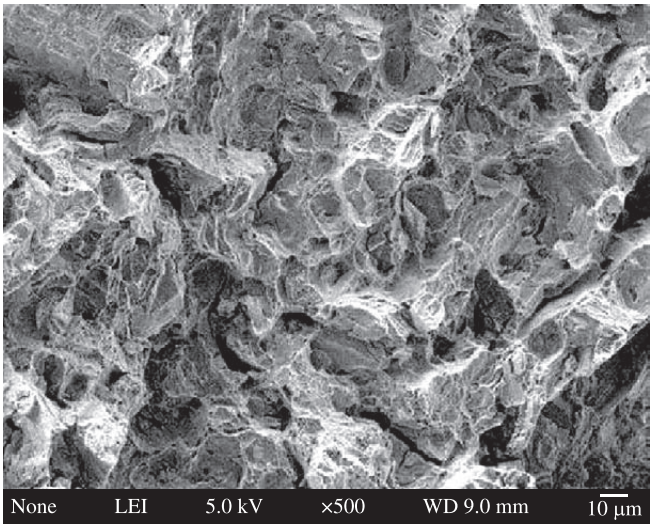

(a)

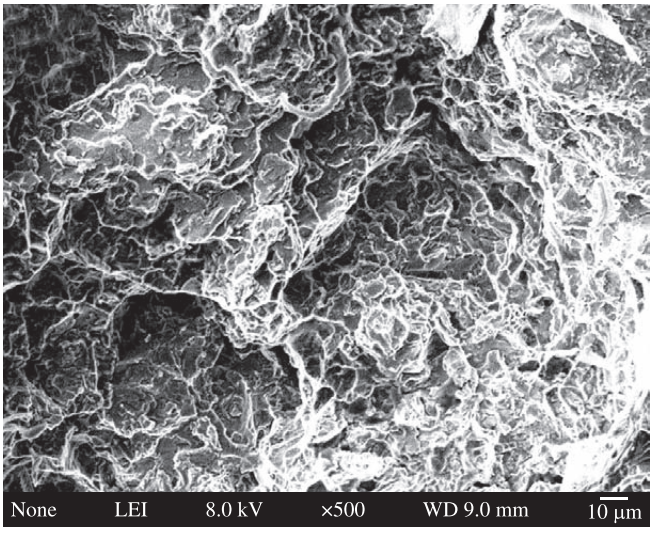

(b)

Figure 13. Fractographs of the AZ91D alloys a) without; and b) with refinement.

$$3C + 4Al = Al_4C_3 \ (\Delta G = 203 \text{ kJ.mol}^{-1}) \quad (3)$$

The formed Al_4C_3 particles has high melting point (about 2100 °C[21]) and are very stable in the melts with temperatures of 650~790 °C. More importantly, the Al_4C_3 compound has same crystal structure of hexagonal close-packed lattice to α-Mg and the smallest crystal mismatch between them is only 3.35%, much less than 15% of the critical value for particles to act as heterogeneous nucleant substrates[27]. Therefore, it can be concluded that the nucleant substrates are believed to be the Al_4C_3 particles.

3.3. Effect of grain refinement on tensile properties

According to the discussion of Section 3.1, a grain refining technique can be obtained: 1% $MgCO_3$ is added into AZ91D alloy melt at 790 °C, followed by cooling to 705 °C in rate of 4.25 °C s^{-1} and pouring. The resulting grain size is only 53 µm for the cast rod with diameter of 16 mm. The result from tensile test indicates that the ultimate tensile strength and elongation of the alloy refined by this technique is 198 MPa and 6% respectively, while those of the un-refined alloy is 164 MPa and 3% respectively (Figure 12). This implies that the obtained grain refining technique has significant refining role for AZ91D alloy and can obviously improve its tensile properties.

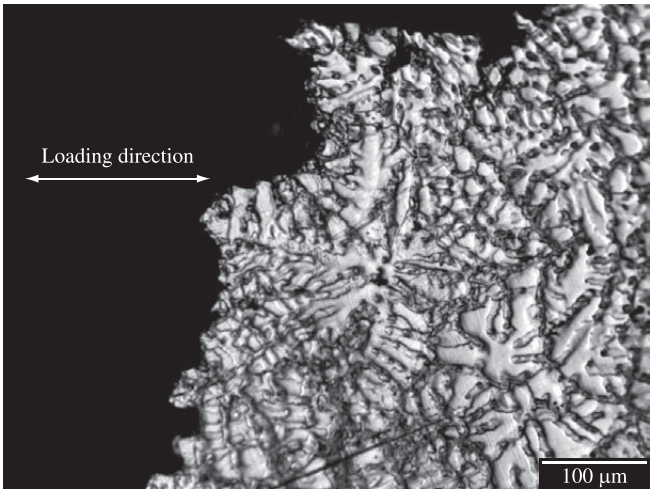

(a)

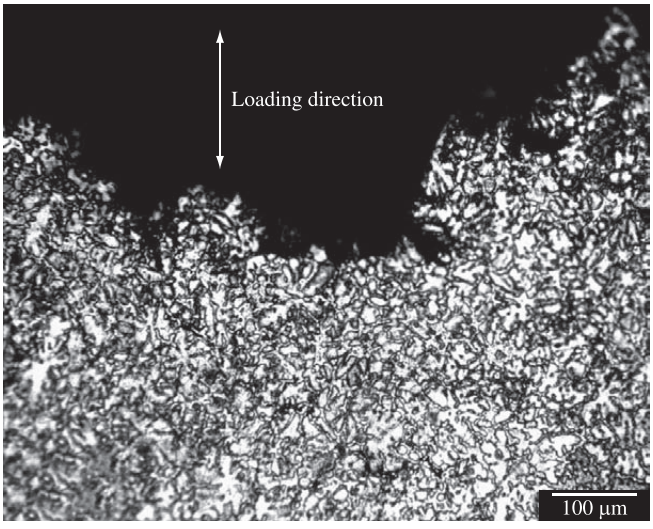

(b)

Figure 14. Microstructures taken near the fracture surfaces along the longitudinal direction of a) un-refined; and b) refined AZ91D alloys.

Figure 13 gives the fracture surface morphologies of these two kinds of alloys. It shows that the morphology of the un-refined alloy displays large crystal salt-like characteristic and there also have some cracks on it, exhibiting brittle fracture features (Figure 13a). But that of the refined alloy reveals a fine microstructure and has relatively ductile fracture characteristics (Figure 13b). From the microstructures taken near the fracture surface along the tensile loading direction, one can be found that the fracture of the un-refined alloy during tensile testing goes along the eutectic structure between the developed dendrites (Figure 14a) while that of the refined alloys operates frequently through the fine equiaxed dendrites (Figure 14b).

It is known that the hard and brittle β phase ($Mg_{17}Al_{12}$) discontinuously distributes in skeleton-shaped irregular particles in interdendritic regions[31]. This distribution must bring out large deleterious effect on deformation harmony during tensile testing and cracks usually form in the β particles due to their breakage. In addition, large numbers of porosities always exist in these regions. So the first formed cracks preferentially propagate along these sites and result in its early fracture and low tensile properties. But for the refined alloy, the size of β particles is decreased (comparing Figure 15a and b) and their distribution becomes more uniform. The harmfulness to the deformation is thereby weakened and the bonding strength between dendrites is improved. So the first formed cracks propagate frequently through the dendrites. Because the primary dendrites belong to a solid solution and it has better plasticity than the β phase, the fracture surface exhibits obvious ductile fracture characteristics.

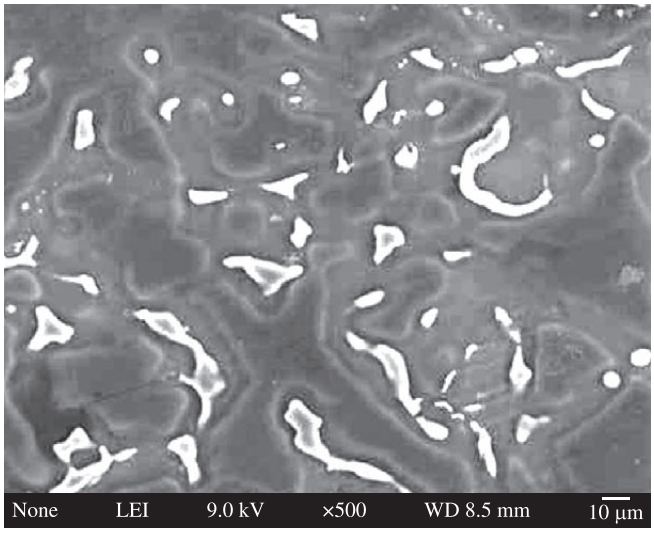

(a)

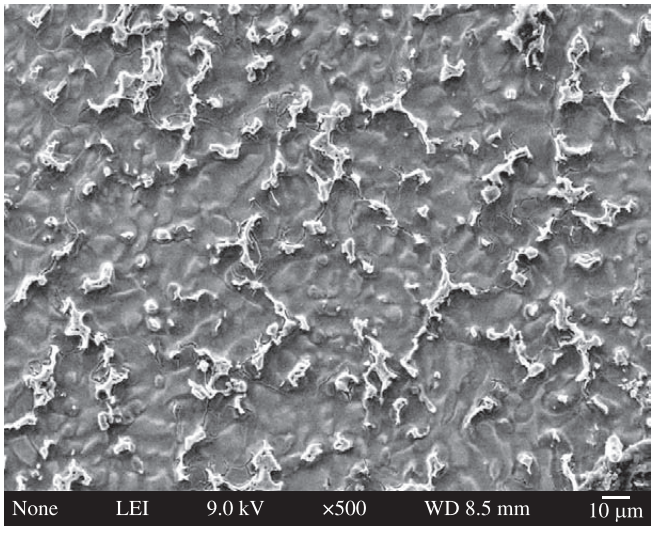

(b)

Figure 15. Microstructures of a) the un-refined; and b) refined AZ91D alloys.

4. Conclusions

1. $MgCO_3$ is an effective grain refiner for AZ91D alloy. The grain size can be decreased from 311 μm of the un-refined alloy to 53 μm.
2. The refining parameters have large effect on the grain size of AZ91D alloy. There is an optimal addition amount of 1% $MgCO_3$ at the addition temperature of 790 °C. As the addition temperature rises or the cooling rate from addition temperature to pouring temperature increases, the grain size decreases.
3. The inoculation fading of $MgCO_3$ is quite quick and obvious, so the melt should be poured as soon as possible.
4. The microstructure sensitivity of the AZ91D alloy treated by $MgCO_3$ to casting thickness is relatively high and the microstructure of cast rod with large diameter is quite nonuniform.
5. The refining mechanism belongs to heterogeneous nucleation and the nucleation substrates are believed to be the Al_4C_3 particles formed from the reactions between the added $MgCO_3$ and molten alloy.
6. The grain refining technique can obviously improve the tensile properties of AZ91D alloy and change the dominative fracture mode from intergranular fracture to transgranular fracture.

Acknowledgements

This work was supported by the National Basic Research Program of China (grant No. G2007CB613706), the Development Program for Outstanding Young Teachers in Lanzhou University of Technology and the Opening Foundation of Key Laboratory of Gansu Advanced Non-ferrous Metal Materials.

References

1. Easton M, Beer A, Barnett M, Davies C, Dunlop G, Durandet Y et al. Magnesium alloy applications in automotive structures. *Journal of the Minerals, Metals and Materials Society - JOM*. 2008; 60:57-62.
2. Eliezer D, Aghion E and Froes FH. Magnesium science, technology and applications. *Advanced Performance Materials.* 1998; 5:201-212.
3. Fan Z. Semisolid metal processing. *International Materials Review*. 2002; 47:49-85.
4. Vinotha D, Raghukandan K, Pillai UTS and Pai BC. Grain refining mechanisms in magnesium alloys – An overview. *Transactions of The Indian Institute of Metals*. 2009; 62:521-532.
5. StJohn DH, Qian M, Easton MA, Cao P and Hildebrand Z. Grain refinement of magnesium alloys. *Metallurgical and Materials Transactions A*. 2005; 36:1669-1679.
6. Cao P, Qian M and StJohn DH. Effect of iron on grain refinement of high-purity Mg-Al alloy. *Scripta Materialia*. 2004; 51:125-129.
7. Cao P, Qian M and StJohn DH. Effect of manganese on grain refinement of Mg-Al based alloys. *Scripta Materialia*. 2006; 54:1853-1858.
8. Song CJ, Han QY and Zhai QJ. Review of grain refinement methods for as-cast microstructure of magnesium alloy. *China Foundry*. 2009; 6:93-103.
9. Wang SC and Chou CP. Effect of adding Sc and Zr on grain refinement and ductility of AZ31 magnesium alloy. *Journal of Materials Processing Technology*. 2008; 197:116-121.

10. Wang YX, Zeng XQ and Ding WJ. Effect of Al-4Ti-5B master alloy on the grain refinement of AZ31 magnesium alloy. *Scripta Materialia*. 2006; 54:269-273.
11. Zhang JH, Wang J, Qiu X, Zhang DP, Tian Z, Niu XD et al. Effect of Nd on the microstructure, mechanical properties and corrosion behavior of die-cast Mg-4Al-based alloy. *Journal of Alloys and Compounds*. 2008; 464:556-564.
12. Hirai K, Somekawa H, Takigawa Y and Higashi K. Effects of Ca and Sr addition on mechanical properties of a cast AZ91 magnesium alloy at room and elevated temperature. *Materials Science and Engineering A*. 2005; 40:276-280.
13. Wang YX, Zeng XQ and Ding WJ. Grain refinement of AZ31 magnesium alloy by titanium and low-frequency electromagnetic casting. *Metallurgical and Materials Transactions A*. 2007; 38:1358-1366.
14. Wang LG, Zhang BF and Guan SK. Effects of RE, B on microstructure and properties of AM60 alloy. *Rare Metals and Materials Engineering*. 2007; 36:59-62.
15. Fu HM, Liu D, Zhang MX, Wang H, Kelly PM and Taylor JA. The development of a new grain refiner for magnesium alloys using the edge-to-edge model. *Journal of Alloys and Compounds*. 2008; 456:390-394.
16. Cao P, Qian M and StJohn DH. Native grain refinement of magnesium alloys. *Scripta Materialia*. 2005; 53:841-844.
17. Gunther R, Hartig C and Bormann R. Grain refinement of AZ31 by SiC_p: theoretical calculation and experiment. *Acta Materialia*. 2006; 54:5591-5597.
18. Easton MA, Schiffl A, Yao JY and Kaufmann H. Grain refinement of Mg-Al (-Mn) alloys by SiC additions. *Scripta Materialia*. 2006; 55:379-382.
19. Zhang MX, Kelley PM, Qian M and Taylor JA. Crystallography of grain refinement in Mg-Al alloys. *Acta Materialia*. 2005; 53:3261-3270.
20. Qian M and Cao P. Discussion on grain refinement of magnesium alloys by carbon inoculation. *Scripta Materialia*. 2005; 52:7415-7419.
21. http://baike.baidu.com/view/488587.htm.
22. Lee J-C, Byun J-Y and Park S-B. Prediction of Si contents to suppress the formation of Al_4C_3 in the SiC_p/Al composite. *Acta Materialia*. 1998; 46:1771-1780.
23. Cui ZX. *Metallography & Heat Treatment*. Beijing, China: China Machine Press; 2004. P. 55.
24. Lu L, Dahle AK and StJohn DH. Grain refinement efficiency and mechanism of aluminium carbide in Mg-Al alloys. *Scripta Materialia*. 2005; 53:517-522.
25. Motegi T. Grain-refining mechanisms of superheat-treatment of and carbon addition to Mg–Al–Zn alloys. *Materials Science and Engineering A*. 2005; 413-414:408-411.
26. Jin QL, Eom J-P, Lim S-G, Park W-W and You B-S. Reply to comments on "Grain refining mechanism of a carbon addition method in a Mg–Al magnesium alloy". *Scripta Materialia*. 2005; 52:421-423.
27. Liu S, Chen Y and Han H. Grain refinement of AZ91D magnesium alloy by a new Mg–50%Al_4C_3 master alloy. *Journal Alloys and Compound.* doi:10.1016/j.jallcom.2009.12. 064.
28. Pei H-B, Xu B-Q and Li Y-F. Study on the thermal decomposition behavior of magnesite in carbothermic reduction extraction process for magnesium in vacuum. *Light Metals*. 2010; (1):46-50.
29. Shih T-S, Chung C-B and Chong K-Z. Combustion of AZ61A under different gases. *Materials Chemistry and Physics*. 2002; 74:66-73.
30. Enrique R-R, Paul FB and Edgar L-C. Influence of carbon on the interfacial contact angle between alumina and liquid aluminum. *Surface and Interface Analysis*. 2003; 35:151-155.
31. Dahle AK, Lee YC, Nave MD, Schaffer PL and StJohn DH. Development of the as-cast microstructure in magnesium–aluminium alloys. *Journal of Light Metals*. 2001; 1:61-72.